Eleventh International Conference on CFD in the Minerals and Process Industries
CSIRO, Melbourne, Australia
7-9 December 2015

CFD SIMULATION OF INDUSTRIAL BUBBLE COLUMNS: NUMERICAL AND MODELLING CHALLENGES AND SUCCESSES

David F. FLETCHER*, Dale D. McCLURE, John M. KAVANAGH and Geoffrey W. BARTON
School of Chemical and Biomolecular Engineering, The University of Sydney, Sydney, NSW 2006, AUSTRALIA
*Corresponding author, E-mail address: david.fletcher@sydney.edu.au

ABSTRACT

Although bubble columns are widely used in many industrial situations, there are very few studies of such devices operating at high superficial velocities. Numerical simulations are reported here across a wide range of operating conditions, where we discuss model assumptions and model validation. Particular emphasis is placed on the various solution methods that can be employed. In particular, we show that massive speed-up is possible using the new NITA solver in ANSYS Fluent 16.

NOMENCLATURE

C_d	drag coefficient
D	diffusion coefficient
d_b	bubble diameter
k	turbulence kinetic energy
$\boldsymbol{M}$	momentum exchange term
p	pressure
S	source term
t	time
T	source term due to presence of bubbles
$\boldsymbol{U}$	velocity
Y	mass fraction
α	volume fraction
ε	turbulence energy dissipation rate
Γ	exchange coefficient
μ	dynamic viscosity
ρ	density

Subscripts

Dis, O2	dissolved oxygen
eff	effective (i.e. laminar + turbulent)
G	gas
L	liquid
O2	oxygen
t	turbulent

INTRODUCTION

Over the last four years, we have embarked on a major project to understand industrial bubble columns used in the fermentation industry. Of central importance is the extension of the existing experimental database and models to high superficial velocities, for which the literature is largely empirical (Heijnen and van't Riet (1988), Kantarci et al. (2005)), and to complex fluids containing biologically active organisms. The challenges are enormous given that the model must be able to predict hold-up, oxygen transfer, mixing times and the impact of these factors on the kinetics of micro-organisms in a system containing a range of surface active compounds. By using a staged approach in which CFD simulations have been validated using data from bench-top experiments (McClure et al. 2013, McClure et al. 2014a,b) and a pilot-scale plant (McClure et al. 2014d, 2015a,b,c,d,e), we have made considerable progress. Despite keeping the model as simple as possible by employing a single bubble size, the need to perform transient averaging over a sufficiently long time to obtain meaningful data means that simulations are necessarily computationally very demanding.

The simulation work has been carried out in ANSYS CFX version 15 which has proved to be very robust and to allow easy extension of the in-built models using the expression language. However, with the release of ANSYS 16, we have recently migrated this model to ANSYS Fluent, using its User Defined Function (UDF) capability. The prime motivation for this was to try out the new non-iterative (NITA) multiphase solver in Fluent which has the potential to speed up computations to the point where industrial-scale bubble column simulations become practical.

Therefore the objectives of this paper are:

1. To provide a complete description of the model developed;
2. Discuss the choice of closure relationships and numerical schemes;
3. Compare the results from ANSYS Fluent against the experimental data and the already published results from ANSYS CFX;
4. Draw some conclusions on the optimum solution approach for the software considered.

MODEL DESCRIPTION

The model is based on the standard shared pressure formulation of the Eulerian multiphase flow equations. We have used a single bubble size based on our measurements of bubble size distributions and the need to keep the simulations manageable in terms of computational cost.

Conservation Equations

The conservation equations for mass, momentum and species for the gas phase are as follows:

$$\frac{\partial(\rho_G \alpha_G)}{\partial t} + \nabla \cdot (\rho_G \alpha_G \boldsymbol{U}_G) = \mathrm{S}_G \qquad (1)$$

$$\frac{\partial(\rho_G \alpha_G)}{\partial t} + \nabla \cdot (\rho_G \alpha_G \boldsymbol{U}_G \otimes \boldsymbol{U}_G) = -\alpha_G \nabla p + \nabla \cdot \left(\alpha_G \mu_{G,\mathrm{eff}} \left[\nabla \boldsymbol{U}_G + (\nabla \boldsymbol{U}_G)^T - \frac{2}{3} \boldsymbol{\delta} \nabla . \boldsymbol{U}_G \right] \right)$$

$$+ \alpha_G \rho_G \boldsymbol{g} + \boldsymbol{M}_{GL} \quad (2)$$

$$\frac{\partial(\rho_G \alpha_G Y_{O2})}{\partial t} + \nabla \cdot \left(\alpha_G \left(\rho_G \boldsymbol{U}_G - \rho_G D_{\text{eff},O2} \nabla Y_{O2}\right)\right) = S_G - \Gamma_{GL} \quad (3)$$

Equations for the liquid phase are readily obtained by swapping 'liquid' for 'gas' and 'dissolved O_2' for 'O_2'.

Turbulence Model

Turbulence in the liquid phase was modelled using the standard *k-ε* model, whilst the dispersed phase zero equation model was used for the gas phase. The transport equations for the turbulence kinetic energy (*k*) and the rate of dissipation of turbulence kinetic energy (*ε*) for the liquid phase are thus:

$$\frac{\partial(\alpha_L \rho_L k_L)}{\partial t} + \nabla \cdot \left(\alpha_L \left(\rho_L k_L \boldsymbol{U}_L - \left(\mu + \frac{\mu_{t,L}}{\sigma_k}\right) \nabla k_L\right)\right) = \alpha_L (P_L - \rho_L \varepsilon_L) + T_{LG,k} \quad (4)$$

and

$$\frac{\partial(\alpha_L \rho_L \varepsilon_L)}{\partial t} + \nabla \cdot \left(\alpha_L \rho_L \varepsilon_L \boldsymbol{U}_L - \left(\mu + \frac{\mu_{t,L}}{\sigma_\varepsilon}\right) \nabla \varepsilon_L\right) = \alpha_L \frac{\varepsilon_L}{k_L} (C_1 P_L - C_2 \rho_L \varepsilon_L) + T_{LG,\varepsilon} \quad (5)$$

where P_L is the turbulence production due to shear. The constants C_1, C_2, σ_k and σ_ε take the standard values of 1.44, 1.92, 1.0 and 1.3, respectively. The terms involving T_{LG} are the sources and sinks of turbulence due to the presence of the bubbles and are presented in the Closure Relationships section.

The turbulent viscosity ($\mu_{t,L}$) is modelled as:

$$\mu_{t,L} = C_\mu \rho_L \left(\frac{k_L^2}{\varepsilon_L}\right) \quad (6)$$

where C_μ was set to 0.09 and no bubble-induced turbulence was modelled as part of the turbulent viscosity. The gas phase turbulent viscosity is determined from

$$\mu_{t,G} = \frac{\rho_G}{\rho_L} \mu_{t,L} \quad (7)$$

Closure Relationships

$\boldsymbol{M}_{GL}$ in eqn. (2) represents the interphase momentum exchange terms. Here, we have modelled interphase drag and turbulence dispersion. Our previous work showed the lift force to be unimportant for the operating bubble size (McClure et al., 2014a). Virtual mass is not included as it has previously been shown to have a small effect (Tabib et al., 2008) and experience is that it reduces model stability markedly.

The drag force per volume ($\boldsymbol{F}_D$) for spherical bubbles is given by:

$$\boldsymbol{F}_D = \frac{3}{4} \frac{C_D}{d_b} \rho_L \alpha_G f(\alpha_G) (\boldsymbol{U}_G - \boldsymbol{U}_L) |\boldsymbol{U}_G - \boldsymbol{U}_L| \quad (8)$$

The drag force experienced by a single bubble was calculated using the Grace model (Clift et al., 1978). The function $f(\alpha_G)$ is included to account for both high voidage effects, which reduce drag, and the effect of surface active components that increase drag. There are relatively few data available in the literature for these functions, so we have previously tuned these parameters against our own experimental data. For the drag reduction due to high voidage, we have used a modified form of the Simonnet et al. (2007) model, whilst for the increase due to surface active components we have used a multiplication factor, so that the function $f(\alpha_G)$ is given by:

$$f(\alpha_G) = \begin{cases} \min(f'(\alpha_G), 1.0) & f'(\alpha_G) > 1 \\ 0.8 f'(\alpha_G) & f'(\alpha_G) < 1 \end{cases}$$

$$f'(\alpha_G) = C_{Ds}(1 - \alpha_G) \times \left[(1 - \alpha_G)^{25} + \left(4.8 \frac{\alpha_{loc}}{1 - \alpha_{loc}}\right)^{25}\right]^{-\frac{2}{25}} \quad (9)$$

where the factor of 0.8 is removed and C_{Ds} is set to 2 if surfactants are present.

Turbulent dispersion was also included, modelled using the Favre-averaged drag relationship implemented in ANSYS CFX and ANSYS Fluent as developed by Burns et al. (2004):

$$\boldsymbol{F}_{TD} = \boldsymbol{M}_{GL,Drag} \frac{\upsilon_{T,L}}{Sc_{t,L}} \left(\frac{\nabla \alpha_G}{\alpha_G} - \frac{\nabla \alpha_L}{\alpha_L}\right) \quad (10)$$

where $\boldsymbol{M}_{GL,Drag}$ is the inter-phase momentum transfer due to drag and $Sc_{t,L}$ is the turbulent Schmidt number for the continuous phase, which has a default value of 0.9.

The model developed by Pfleger and Becker (2001) was used in our previous work using ANSYS CFX for the turbulence production due to the relative motion of the bubbles. In this model

$$T_{LG,k} = \alpha_L C_1 |\boldsymbol{M}_{LG}| |\boldsymbol{U}_G - \boldsymbol{U}_L| \quad (11)$$

and

$$T_{LG,\varepsilon} = C_5 \frac{\varepsilon}{k} \alpha_L C_1 |\boldsymbol{M}_{LG}| |\boldsymbol{U}_G - \boldsymbol{U}_L| \quad (12)$$

where C_5 was set to a value of 1.0. The inclusion of bubble-induced turbulence production proved essential to obtaining meaningful results, as without it both voidage and velocity predictions were very poor (McClure at al., 2014a).

Whilst we found this model to be stable in ANSYS CFX, we were unable to code it in a stable manner in ANSYS Fluent. The ε source term is proportional to ε/k and it was observed that ε increased rapidly, leading to massive dissipation of k and consequently an increase in ε, which always led to divergence of the ε equation. ANSYS Fluent has in-built the model of Trosko and Hassan, (2001) which is similar to that of Pfleger and Becker but the source for the ε equation here uses a bubble pseudo-turbulence dissipation frequency to replace ε/k ratio in eqn. (12) as follows:

$$\frac{\varepsilon}{k} \equiv \left(\frac{2 C_{vm} d_b}{3 C_d |\boldsymbol{U}_G - \boldsymbol{U}_L|}\right)^{-1} \quad (13)$$

where the characteristic time for turbulence destruction due to the presence of bubbles is determined using the

bubble residence time rather that the eddy time-scale. This model requires the inclusion of an added mass term to provide the added mass coefficient C_{vm}.

After reviewing the literature, the model of Yao and Morel (2004) was implemented and found to be stable in both ANSYS CFX (where it is available as a beta feature) and ANSYS Fluent. In this model, the characteristic time is determined using a length-scale from the bubble diameter by making the following replacement for the ε source in eqn. (12)

$$\frac{\varepsilon}{k} \equiv \left(\frac{\varepsilon}{d_b^2}\right)^{\frac{1}{3}} \qquad (14)$$

and C_1 and C_5 are set to 1 in equations (11) and (12). Simulations in ANSYS CFX showed that this model and that of Pfleger and Becker gave very similar results.

Mass Transfer

The movement of O_2 from the gas phase to the liquid was modelled using diffusion-limited mass transfer, assuming equilibrium conditions at the liquid-bubble interface. There was assumed to be no resistance on the gas side and a mass transfer coefficient k_L of 4×10^{-4} m s^{-1}, derived from our experimental work and used in the literature (Krishna and van Baten, 2003), was applied on the liquid side. A Henry's law constant of 77942 Pa m^3 mol^{-1} was used. A sink term of the form $-C_{sink}Y_{Dis,O2}\rho_L$ was applied to the dissolved oxygen equation, with C_{sink} set to a value of 10^5 s^{-1}. This is added to mimic the fast cobalt-catalyzed sulphite reaction used in our experiments to consume the dissolved oxygen and maintain a mass transfer driving force (McClure et al., 2015b).

NUMERICAL METHODS

ANSYS CFX uses a vertex-based scheme in which a polyhedral mesh is built around each vertex. The resultant equations are solved using a coupled solver that links the equations for the velocities and pressures. In multiphase flow this is known as the segregated volume fraction solver, as the volume fraction equations are solved outside of this system. It also has an option, termed the coupled volume fraction solver, in which the volume fraction equations are included in the coupling with the pressure and velocities. This has been shown to be beneficial in many circumstances, particularly when added mass or similar terms involving volume fractions are to be integrated into the momentum equations.

By default, ANSYS CFX uses a bounded second-order scheme for the convective terms, except for the turbulence equations for which a first-order scheme is used. A second-order backward Euler scheme is used for the transient term. Iteration is performed at each time-step and typically 2-5 coefficient loops are required to reduce the normalized residuals to 10^{-4}.

ANSYS Fluent uses a cell-centred scheme and offers a number of different approaches to solve the multiphase flow equations. The most widely used is the PC-SIMPLE scheme, which is a modification of the SIMPLE algorithm widely used in single phase flow, in which the pressure and velocity equations are still solved in a segregated manner but the velocities of all phases are coupled. This means that the coupling between phases is strong and the drag force term is always kept in balance. ANSYS Fluent also has coupled solvers, based on those in ANSYS CFX, that can include or exclude the volume fraction equations as desired.

When any of the above solvers are used in transient mode the matrix equations are formulated and then the linear solvers are applied to obtain an approximate solution which is then used to update the coefficient matrix with the process being repeated until convergence is obtained. This is known as an iterative solver. It can be computationally very expensive, as typically 3-8 iterations might need to be done at each time-step using a coupled solver or 10-20 iterations using PC-SIMPLE, and calculation of the matrix coefficients is computationally intensive. This load could obviously be reduced if the matrix coefficients were calculated only once, which is the idea behind the non-iterative (NITA) solver.

The NITA solver is available with the PC-SIMPLE scheme in ANSYS Fluent 16 and later versions. Initially the velocity field is determined to a suitable convergence level, then the pressure correction step and the velocity pressure flux correction steps are solved. These operations are done in a split manner in such a way that errors are reduced to the level of the truncation error, rather than attempting to reduce the splitting error to zero as is done in the iterative solver. Clearly this comes at a price and it is required that the time step is small enough that the residuals can be reduced sufficiently at each step for a converged solution to be obtained. However, for typical Eulerian multiphase flows a small time step is usually required anyway so this is not a stringent requirement.

In the ANSYS Fluent simulations the gradients were calculated using the least-squares option, the QUICK scheme was used for momentum and volume fractions, second-order upwind for species and scalars, and first-order for turbulence equations. The first-order time-stepping scheme was applied, whilst all under-relaxation factors are automatically set to unity when the NITA scheme is invoked. It should be noted that as of version 16.1 if user defined scalars are used the NITA scheme cannot be used which means the ITA scheme had to be used for the tracer calculations described below. However, in later work we have used mass fractions in place of scalars to circumvent this limitation.

The additional models for bubble drag enhancement, turbulence generation, dissolved oxygen uptake and tracer injection were implemented using the User Defined Function (UDF) capabilities of ANSYS Fluent.

RESULTS

The models developed in ANSYS CFX and ANSYS Fluent were compared with the published data from the pilot-plant experiments published in McClure et al. (2015b,c). This bubble column is 2 m in height and 0.39 m in diameter. Air was introduced through a 'tree' type sparger at superficial velocities between 0.14 and 0.28 m s^{-1}, the centre-line of the sparger being located 0.135 m above the base of the cylindrical section of the column. The sparger used in this work had orifices 0.5 mm in diameter, and a free area of 2.2%.

Initial model validation was performed for an air-water system to ensure simulation results were consistent with both those obtained experimentally and with those from

ANSYS CFX. The liquid density was set to 997 kg m^{-3}, the liquid viscosity to 0.00089 Pa s, the air density to 1.185 kg m^{-3} and the air viscosity to 1.831×10^{-5} Pa s. In line with the experimental data, the bubble size was set to 8 mm and not varied as a function of depth as the induced change was negligibly small.

For the simulations performed to study oxygen mass transfer, the water contained surfactants and the liquid used has a density of 998 kg m^{-3} and a viscosity of 0.0015 Pa s. Based on our experimental data, a fixed bubble size of 4 mm was used in all calculations.

The same computational mesh, comprising 36,000 hexahedral cells, as used in the ANSYS CFX simulations was applied here. This mesh density was shown to give an adequate representation in the ANSYS CFX simulations (McClure et al., 2014c). A fixed timestep of 1 ms was used in all simulations.

Air-water voidage and velocity profiles

The first validation test compared profiles of local void fraction and liquid velocity across the vessel for a superficial velocity of 0.16 m s^{-1}. Both simulations used the Yao and Morel bubble-induced turbulence model and the drag enhancement function given in eqn. (9) with $C_{Ds} = 1$.

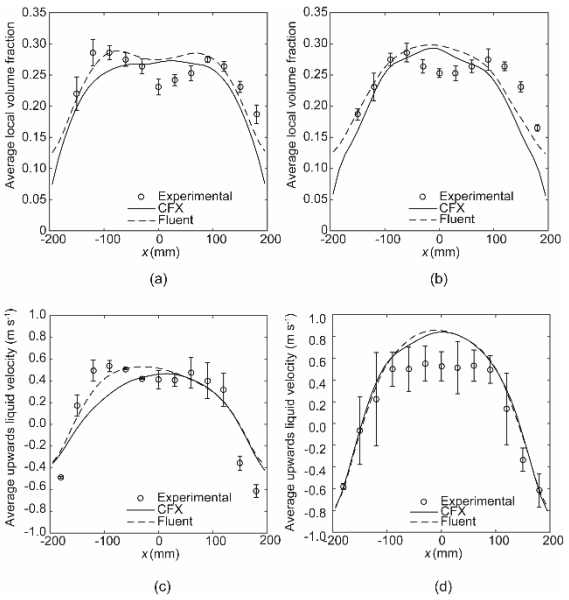

Figure 1: Plots showing the local volume fraction and average upwards liquid velocity. The top row (a) and (b) are hold-up profiles at heights of 550 mm (a) and 1050 mm (b) above the base of the column; while the bottom row shows profiles of the average upwards liquid velocity at (c) 550 mm above the base of the column and (d) 1050 mm above the base of the column.

It is evident from Fig.**Figure 1** that both ANSYS CFX and ANSYS Fluent give very similar results and that these are close to the experimental data. This is a representative comparison and is typical of the level of agreement observed between the experimental data and the two CFD results. This provides an excellent cross check of the hydrodynamics simulations and, in particular, the implementation of the drag law and turbulence enhancement models.

Tracer simulations

Simulations were also performed to study mixing times within the column. In ANSYS CFX simulations, tracers were injected using a point source over a period of 1 s at various locations and the simulation was then run, starting from a solution that had been run for 120 s, until the tracer concentration reached within 5% of the final equilibrium value. By using multiple tracers in the same simulation, all tracers 'saw' the same column hydrodynamics. In ANSYS Fluent, point sources are not available, so a small group of cells were identified over which the injection could be performed with the concentration level being adjusted so that the total injected mass was the same at each injection point.

A comparison between the results from the two models and the experimental data is shown in Fig. 2. The results are for superficial velocities of ~0.17 m s^{-1}. The ANSYS CFX simulations used the bubble-induced turbulence model of Pfleger and Becker whilst the ANSYS Fluent simulations used the model of Yao and Morel. The ANSYS Fluent simulations used the PC-SIMPLE iterative solver as the NITA solver cannot be used with User Defined Scalars (UDSs) enabled.

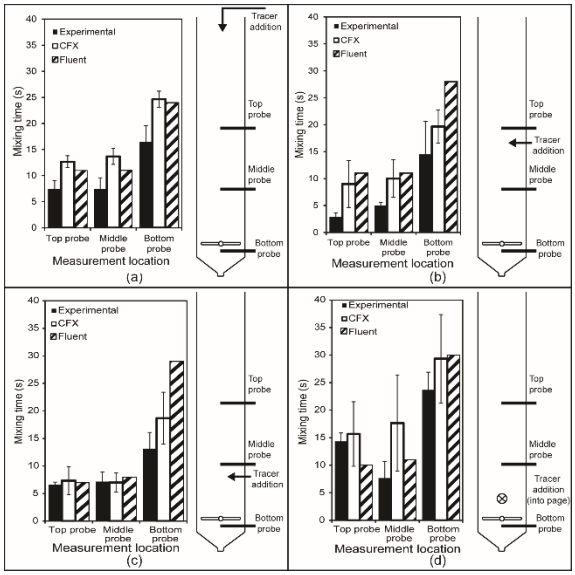

Figure 2: Mixing time simulation results for the tracer added: (a) at the free surface, (b) 850 mm above the base of the column, (c) 350 mm above the base of the column and (d) 200 mm above the base of the column. The probe and injection locations are shown in the schematic next to each dataset.

It is evident from Fig. 2 that the results are very similar between the two models and our experimental data. The error bars on the experimental data and ANSYS CFX results show the range of values obtained for three repeat injections, whereas the ANSYS Fluent simulations are for a single injection. Again, there are no systematic differences between the three sets of data.

Simulations for the system with sodium sulphite

The remaining simulations presented here are for the system containing sodium sulphite that acts as a surfactant and the oxygen scavenger. All simulations used the bubble drag law shown in equation (9) with $C_{Ds} = 2$. The ANSYS CFX simulations used the Pfleger and Becker model for

bubble-induced turbulence, whereas the ANSYS Fluent simulations used the alternative model of Yao and Morel.

Overall Hold-up

The experimental data for overall hold-up are compared with simulation results in Fig. 3.

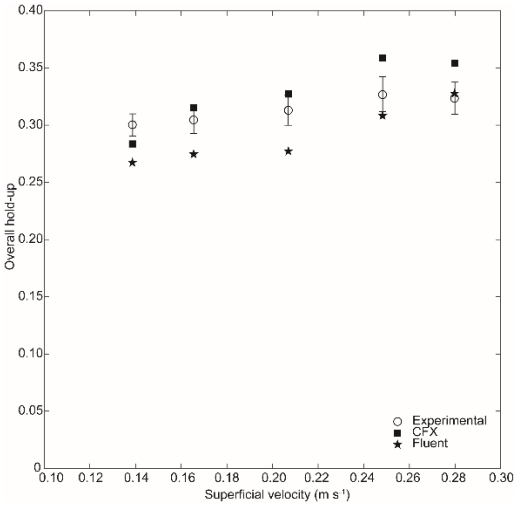

Figure 3: Overall hold-up as a function of superficial velocity for the surfactant containing system.

Both simulations capture the correct experimental trend. The ANSYS CFX results are a little closer at the lower superficial velocities, whilst the ANSYS Fluent results are a little better at higher values. These differences are likely caused by differences in the bubble-induced turbulence model and their implementation.

Oxygen Transfer Rate

A comparison of the oxygen transfer rate (OTR) is given in Fig. 4. Once again, results from the two models give an acceptable level of agreement with the experimental data which have a scatter which is larger than the differences between the two simulation results.

COMPUTATIONAL PERFORMANCE

Once the transient averaging had been performed for 100 s of real-time, the 0.21 m s^{-1} superficial velocity case was used to collect data on computational performance. 50 additional iterations were performed using a variety of solver settings. The simulations used a 3.2GHz Intel i7 processor having 32 GB RAM and used ANSYS 16.1 as this has the most up to date solvers. Table 1 gives a summary of the results obtained.

It is evident from Table 1 that there is a huge speed-up to be gained from using the NITA solver in ANSYS Fluent. It is 4.3 times faster than using the PC SIMPLE solver of ANSYS Fluent; 22-25 times faster than using the coupled solver in ANSYS Fluent or in ANSYS CFX. In short, ANSYS CFX simulations that were taking around 3 weeks to perform are being completed in a day using ANSYS Fluent and the NITA solver.

DISCUSSION

The CFD model used here is the simplest possible that captures (in a meaningful way) all mechanisms known to be important in bubble column behavior. It clearly has a number of limitations that need outlining.

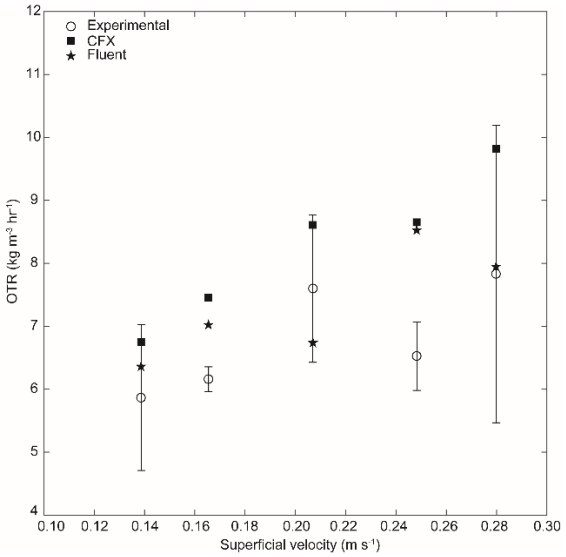

Figure 4: OTR as a function of superficial velocity for the surfactant containing system.

Solver	Cores	Algorithm	Time (s)	Relative timing
Fluent	4	NITA	21.4	1
Fluent	2	NITA	35.5	1.7
Fluent	1	NITA	60.0	2.8
Fluent	4	PC SIMPLE	92.6	4.3
Fluent	4	Coupled, momentum only	186.3	8.7
Fluent	4	Coupled, momentum and volume fraction (VF)	481.3	22.5
CFX	4	Coupled, VF segregated	484	22.6
CFX	4	Coupled, inc. VF	519	24.3

Table 1: Simulation timings for different solver methods and numbers of cores.

Firstly, the use of single bubble size is obviously a gross simplification. It is in principle straightforward, although computationally expensive, to enable the MUSIG approach in ANSYS CFX or the Population Balance or Method of Moments models in ANSYS Fluent. However, there are very significant differences in the various models for bubble coalescence and breakup even for simple air-water or steam-water systems proposed in the published literature, and we have found nothing for systems that contain the surface active components found in industrial bubble column systems. In this context, the point should be made that the measured bubble size distribution for industrial fermentation media is much narrower than for an air-water system due to the surfactants present.

Secondly, the impact of drag reduction in bubble swarms and the drag increase for systems with surface active components is poorly understood. The literature is sparse and we were compelled to make empirical adjustments in order to obtain results consistent with our experiments,

noting that with no drag reduction as a function of voidage the holdup is massively over-predicted.

Thirdly, inclusion of turbulence generation due to the bubbles plays an important role in obtaining physically sensible results. The literature contains many different forms for this term, as seen in eqns. (11)-(14). A fundamental study to tie down the correct form of this term for high superficial velocity and high voidage flows would be most useful in seeing our modeling efforts extended into other areas of industrial importance.

CONCLUSIONS

A computationally-efficient CFD model has been described that can be used to study the behavior of a bubble column operating at high superficial velocities. Results have been validated against pilot-scale data for both air-water and surfactant containing systems. Whilst agreement is not perfect, all important trends are adequately captured, and this work has identified the key areas likely to further improve the level of agreement between modelling and experimental results.

A key result from this work is that the NITA solver in ANSYS Fluent can reduce run-times by a factor of (up to) 25 over the coupled solvers in ANSYS CFX and ANSYS Fluent, and some 4 times that of the PC-SIMPLE solver in ANSYS Fluent. This is hugely significant in terms of the mesh resolution that can be used and the number of simulations that can be performed given the transient nature of bubble column behaviour.

ACKNOWLEDGEMENTS

The authors gratefully acknowledge that this work was partially funded by ARC Linkage Grant LP120100608. DFF thanks Mohan Srinivas and Shitanshu Gohel of ANSYS India for their assistance in developing the UDFs.

REFERENCES

BURNS, A.D., FRANK, T., HAMILL, I. and SHI, J.-M., (2004), "The Favre averaged drag model for turbulent dispersion in Eulerian multi-phase flows", *Proc. 5th International Conference on Multiphase Flow*, Yokohama, Japan, May 30 – June 4.

CLIFT, R., GRACE, J.R. and WEBER, M.E., (1978), Bubbles, Drops and Particles, Academic Press, New York.

HEIJNEN J. J. and van't RIET, K., (1984), "Mass transfer, mixing and heat transfer phenomena in low viscosity bubble column reactors", (1984), *Chem. Eng. J.*, **28**, 21-42.

KANTARCIA, N., BORAKB, F., and ULGENA, K.O., (2005), "Bubble column reactors", *Process Biochem.*, **40**, 2263–2283.

KRISHNA, R. and van BATEN, J. M., 2003. "Mass transfer in bubble columns", *Catalysis Today*, **79-80**, 67-75.

McCLURE, D.D, KAVANAGH, J.M., FLETCHER, D.F. and BARTON, G.W., (2013), "A contribution towards the development of a CFD model of bubble column bioreactors: Part One – A detailed experimental study", *Chem. Eng. Technol.*, **36**(12), 2065-2070.

McCLURE, D.D, KAVANAGH, J.M., FLETCHER, D.F. and BARTON, G.W., (2014a), "Development of a CFD model of bubble column bioreactors: Part Two – Comparison of experimental data and CFD predictions", *Chem. Eng. Technol.*, **37**(1), 131-140.

McCLURE, D.D, DELIGNY, J., KAVANAGH, J.M., FLETCHER, D.F. and BARTON, G.W., (2014b), "An investigation into the impact of surfactant chemistry on bubble column systems", *Chem. Eng. Technol.*, **37**(4), 652-658.

McCLURE, D.D, NORRIS, H., KAVANAGH, J.M., FLETCHER, D.F. and BARTON, G.W., (2014c), "Validation of a computationally-efficient CFD model for industrial bubble column bioreactors", *Ind. Eng. Chem. Res.*, **53**(37), 14526-14543.

McCLURE, D.D, ABOUDHA, N., KAVANAGH, J.M., FLETCHER, D.F. and BARTON, G.W., (2015a), "Mixing in bubble column reactors: Experimental study and CFD modelling", *Chem. Eng. J.*, **264**, 291-301.

McCLURE, D.D, LEE, A.C., KAVANAGH, J.M., FLETCHER, D.F. and BARTON, G.W., (2015b), "An investigation into the impact of surfactant addition on oxygen mass transfer in a bubble column", *Chem. Eng. Technol.*, **38**(1), 44-52.

McCLURE, D.D, NORRIS, H., KAVANAGH, J.M., FLETCHER, D.F. and BARTON, G.W., (2015c), "Towards a CFD model of bubble columns containing significant surfactant levels", *Chem. Eng. Sc*i., **127**(5), 189-201.

McCLURE, D.D, KAVANAGH, J.M., FLETCHER, D.F. and BARTON, G.W., (2015d), "Calculation of liquid film mass transfer coefficients (k_L) in two-phase mixtures", *Chem. Eng. Technol.*, **38**(4), 571-573.

McCLURE, D.D, KAVANAGH, J.M., FLETCHER, D.F. and BARTON, G.W., (2015e), "Towards a CFD model of bubble columns containing significant surfactant levels", *Chem. Eng. J.*, **280**, 138-146.

PFLEGER, D. and BECKER, S., (2001), "Modelling and simulation of the dynamic flow behaviour in a bubble column", *Chem. Eng. Sci.*, **56** (4), 1737-1747.

SIMONNET, M., GENTRIC, C., OLMOS, E. and MIDOUX, N., (2007), "CFD simulation of the flow field in a bubble column reactor: Importance of the drag force formulation to describe regime transitions", *Chem. Eng. Sci.*, **62**(3), 858-866.

TABIB, M.V., ROY, S.A. and JOSHI, J.B. (2008), "CFD simulation of bubble column–An analysis of interphase forces and turbulence models", *Chem. Eng. J.* **139**(3), 589-614.

TROSKO, A.A. and HASSAN, Y.A., (2001), "A two-equation model turbulence model of turbulent bubbly flows", *Int. J. Multiph. Flow*, **27**, 1965-2000.

YAO, W. and MOREL, C., (2004), "Volumetric interfacial area prediction in upward bubbly two-phase flow", *Int. J. Heat Mass Trans.*, **47**, 307-328.

